R. S. Lakes
Department of Engineering Physics,
Engineering Mechanics Program; Biomedical
Engineering Department,
Materials Science Program and Rheology
Research Center,
147 Engineering Research Building,
1500 Engineering Drive,
University of Wisconsin-Madison,
Madison, WI 53706-1687
e-mail: lakes@engr.wisc.edu

S. Kose

H. Bahia

Department of Civil and Environmental
Engineering,
1415 Engineering Drive, B243 Engineering Hall,
University of Wisconsin-Madison,
Madison, WI 53706-1687

Analysis of High Volume Fraction Irregular Particulate Damping Composites

Concentrated suspensions of inclusions occur in asphalt and dental composite resins. Concentrated suspensions are also of use in achieving a combination of high stiffness and loss (the product E tan δ), desirable in damping layer and structural damping applications. For realizable particulate microstructures, analytical solutions for monodisperse inclusion morphologies such as spherical, random fibrous and platelet, are valid only in the case of a dilute concentration of inclusions. Finite element analyses were conducted of hierarchical particulate composites with high volume fractions of particles of irregular shape. For particle volume concentration 40 percent or less, the results are close to the Hashin-Shtrikman lower formula in a stiffness versus concentration plot and in a stiffness loss map. For larger concentration, stiffness is higher and E tan δ is lower. The irregular particle shape therefore enhances stiffness at a given concentration, and reduces damping layer performance. [DOI: 10.1115/1.1448923]

I Introduction

Composite material properties depend upon the *shape* of the heterogeneities, upon the *volume fraction* occupied by them, and upon the *interface* between the constituents. As for microstructures which are easily realizable, analytical solutions are available for various inclusion morphologies including spherical, fibrous and platelet. These solutions are valid only in the case of a dilute concentration of inclusions. A high concentration of inclusions (i) has advantages in the context of stiff, high damping composites, (ii) occurs in dental composites, and (iii) occurs in asphalt mixtures. Arbitrarily high concentrations can be handled by the hierarchical Hashin-Shtrikman coated spheres morphology by a hierarchical laminate, or specific micro-mechanical analyses [1]. The coated sphere structure contains spherical elements of all sizes, down to the infinitesimal. The hierarchical laminate contains laminations within laminations. In the physical world, one is limited by the size of atoms, therefore such idealized structures cannot be fabricated. Nevertheless, composites with multiple length scales are of interest in both the technological and biological contexts.

As for viscoelastic composites, the loss tangent $\tan\delta = \mathrm{Im}(E^*)/\mathrm{Re}(E^*)$ is a measure of damping and is defined as the ratio of the imaginary part to the real part of the complex modulus E*. The angle δ is the phase angle between stress and strain sinusoids. Tan δ is proportional to the energy loss per cycle within the framework of linear viscoelasticity.

Mechanical damping in materials, whether they be homogenous or composite, is of considerable importance in that one can damp unwanted vibrations in mechanical systems. The product $|E^*|\tan\delta$, is a figure of merit for materials used as damping layers. Figure 1 shows a stiffness-loss map, $|E^*|$ vs. $\tan\delta$, of common materials. Also shown is behavior of asphalt derived from a master curve [2] of modulus and tan δ vs. effective frequency. Structural materials occupy positions to the left or far to the left in the diagram. Selected composite microstructures give rise to high stiffness combined with high loss tangent [3]; such a combination is most easily achieved if the stiff phase is as stiff as possible [4]. Creep is related to mechanical damping by a Fourier integral; if damping is relatively small, the loss tangent is proportional to the slope of the creep curve $J(t)$ on a log log scale.

As for bounds on composite properties, the Hashin-Shtrikman formulas provide upper and lower bounds for stiffness versus volume fraction of elastic isotropic composites of arbitrary microstructure. Specifically, the Hashin-Shtrikman formula [5] for the lower bound on the elastic shear modulus G_L of an *elastic* isotropic composite is as follows.

$$G_L = G_2 + \frac{V_1}{\dfrac{1}{G_1 - G_2} + \dfrac{6(K_2 + 2G_2)V_2}{5(3K_2 + 4G_2)G_2}} \tag{1}$$

K_1, K_2, G_1, and V_1, and G_2 and V_2 are the bulk modulus, shear modulus and volume fraction of phases 1, and 2, respectively. Here $G_1 > G_2$. Interchanging the numbers 1 and 2 in Eq. (1) results in the upper bound G_U for the shear modulus.

For viscoelastic composites, the moduli become complex following the elastic-viscoelastic correspondence principle [6]. The Hashin-Shtrikman ''lower'' curve appears in the upper right on a stiffness-loss map, and is close to the Reuss curve on the same map. Anisotropy in viscoelastic composites with arbitrary volume fraction consequently differs in its effects from elastic composites with fixed volume fraction [2]. In particular, anisotropy does not significantly expand the stiffness loss map. By contrast, in a plot of stiffness vs. volume fraction for elastic composites, a substantial gain in stiffness for a given volume fraction can be achieved by introducing anisotropy. Bounds [7] for viscoelasticity in a stiffness-loss map either coincide with the Hashin-Shtrikman formulas or they are close to them [8,9].

High volume fractions of inclusions can be attained by using multiple inclusion sizes, referred to as hierarchical or polydisperse, by using polyhedral shapes capable of closer packing than spheres, or both. Asphalt and dental composites are examples of particulate composites with high volume fraction of irregular particles. Composites with a high concentration of irregular particulate inclusions are therefore of broad technological interest.

Asphalt mix is a composite of petroleum products, called binder, as a matrix and irregular particles of different size of rock, called aggregate, as inclusions (Fig. 2(*a*)). The matrix is usually produced via vacuum distillation of petroleum crude oils. The irregular particulate inclusions have a high volume fraction, there-

Contributed by the Materials Division for publication in the JOURNAL OF ENGINEERING MATERIALS AND TECHNOLOGY. Manuscript received by the Materials Division July 2, 2001; revised manuscript received September 26, 2001. Associate Editor: S. Mall.

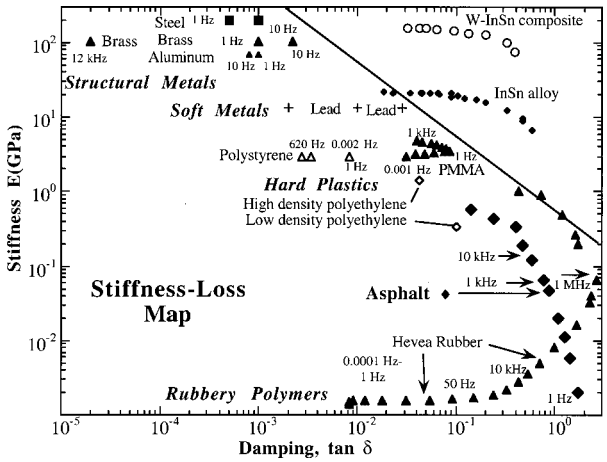

Fig. 1 Stiffness-loss map of common and high performance materials, adapted from [25], with data added based on [1]

II Methods

Image Acquisition and Processing. Input morphological data were taken from an image of asphalt. Image acquisition of hot mix asphalt (HMA) cross-sections was done via a scanner. The scanned images are gray scale pictures that contain 256 shades of gray. One such image of asphalt, is shown in Fig. 2, which also shows the structure of a dental composite and an idealized hierarchical coated spheres morphology which gives rise to the Hashin-Shtrikman bounds for the bulk modulus. For the purposes of generating FEM models, the gray scale image was converted into a binary image that has only two colors, black and white. Following the usual convention "all the pixels" belonging to an aggregate particle were made white and those that belong to the background were made black. To accomplish this a threshold criterion was applied to the gray scale image. The histogram data were obtained using MATLAB software. The process involves counting how many times each of the gray shade values (in a range 0–255) occurs in an image. For asphalt images the threshold value was chosen to be very close to the bottom of the valley (Fig. 3) in its histogram. Asphalt images usually have histograms that are bimodal in nature, that is, the histogram consists of two

fore analytical models for dilute suspensions of particles are not applicable. Asphalt behaves as a viscoelastic liquid or uncrosslinked polymer with a shear modulus of about $G_0 = 1$ GPa in the glassy regime of high frequency and low temperature [1]. In the terminal regime (10^{-6} to 10^{-7} Hz at 15°C) the loss angle δ tends to $\pi/2$. The behavior of asphalt is approximated by time-temperature superposition. Temperature dependence of the mean relaxation times follows an Arrhenius law (from −10°C to 30°C). Activation energies are from 125 to 258 kJ/mole. For temperatures above about 45°C, deviations from time-temperature superposition occur. Such behavior is similar to that seen in polymers. Asphalt binders within hot mix asphalt are distributed in interconnected domains of various geometric dimensions combined with air voids and mineral fine particles that are distributed randomly in this complex composite. A variety of numerical methods have been proposed to treat asphalt [10–12].

Dental composite resins consist of a polymer matrix and stiff inorganic inclusions. The particles in many dental composites are very angular in shape (Fig. 2(*b*)). The inorganic inclusions confer a relatively high stiffness and high wear resistance on the material. Since the composites are translucent they resemble the natural tooth structure. The inorganic inclusions are typically barium glass or silica [quartz, SiO_2]. The matrix typically consists of a polymer such as BIS-GMA. The initial constituents are mixed, then placed in the prepared cavity to polymerize. In view of the greater density of the inorganic particulate phase, a representative 77% by weight of particles corresponds to a volume concentration of about 55% [13], a high concentration. Young's moduli of selected dental composites are typically from 10 to 16 GPa [14]. Shear moduli are 3.3 GPa to 11.2 GPa and $\tan\delta$ at low audio frequency is 0.035 to 0.058 depending on the composite [15].

In the present study, the effects of high concentrations of irregular shape particles are explored. The analysis is considered applicable to such composites as asphalt, dental composite resins, and novel composites intended for high performance damping layers. A digital image of a representative asphalt structure is obtained and processed to distinguish particle and matrix. A finite element method is used to deal with the irregularity of the inclusion shape. An erosion method is then applied to systematically vary the volume fraction. The finite element analysis is repeated at each volume fraction. The elastic-viscoelastic correspondence principle is then applied to the stiffness versus volume fraction results to obtain viscoelastic properties. These properties are compared with the Hashin-Shtrikman formulas on a stiffness-loss map: a diagram of modulus versus viscoelastic loss tangent.

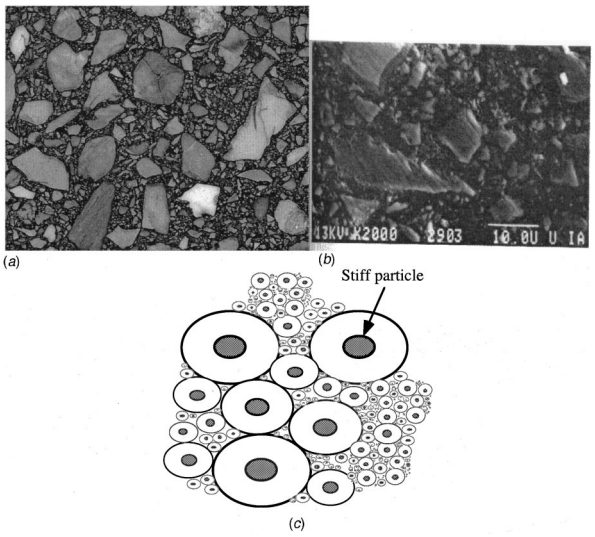

Fig. 2 (*a*) Image (32×43 mm) of asphalt structure. (*b*) Image of dental composite structure [12]. Scale mark: 10 μm. (*c*) Coated spheres morphology which attains exactly the Hashin-Shtrikman bounds for bulk modulus.

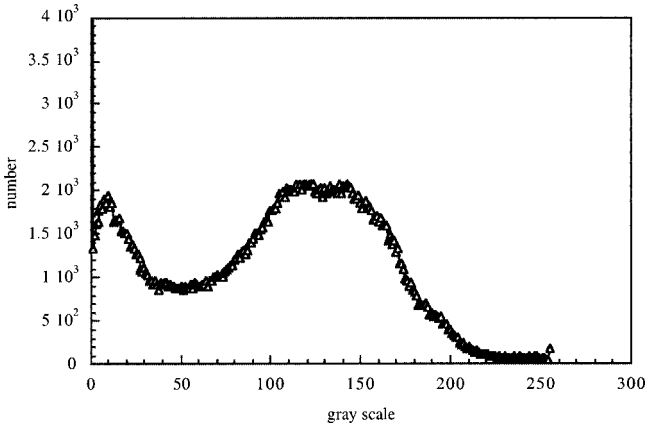

Fig. 3 Histogram of image gray scale. Number of occurrences vs. gray scale value.

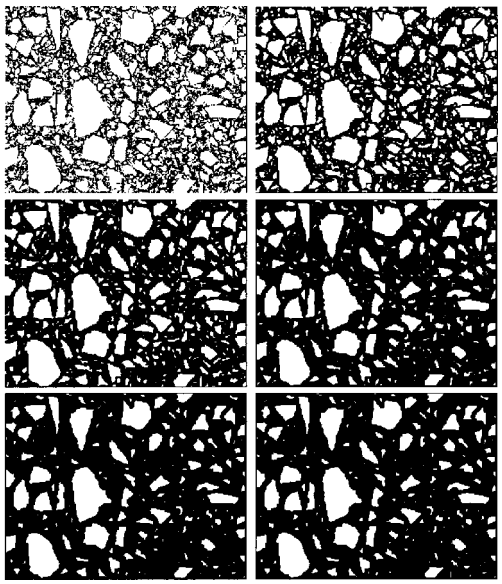

Fig. 4 Creation of models of different volume fraction by erosion of layers from surfaces in the original scanned image

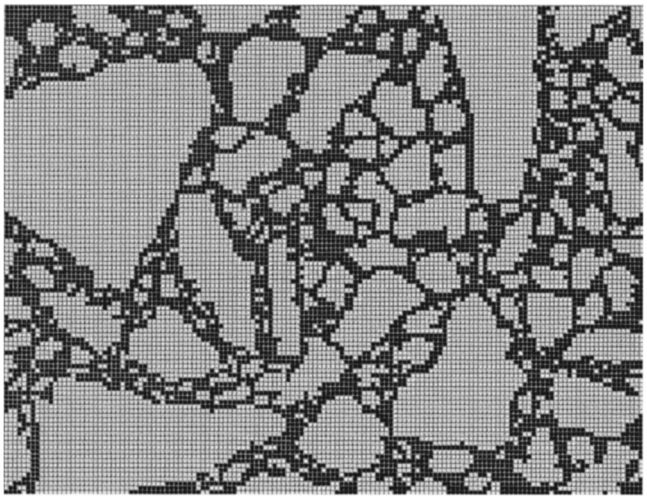

Fig. 5 Magnified view of a portion of the finite element mesh for the smallest particles. The full mesh contains 344,064 elements.

main hills and a valley. The objective is to find the lowest point of the valley. It can be found either manually or automatically. A polynomial was fit to the histogram data. The lowest point of the valley was determined by finding the appropriate local minimum. Once this was accomplished, the histogram was divided into two parts, namely background and foreground population. For each of the populations a normal distribution was found and plotted. The intersection of the two normal distributions is taken to be the optimum threshold. Although this technique is used successfully for thresholding for other classes of images, it was not as successful when applied to asphalt images. One of the most important factors may be the fact that in a asphalt image, populations do not have normal distribution. Several other auto-thresholding algorithms were tried including clustering, entropy, metric, moments, and inter-class variance. None of these were successful in producing an appropriate threshold value for asphalt cross-sectional images. As a result, the method followed in this paper for thresholding is to use the bimodal histogram as a guide and adjust the threshold value visually by comparing the original image with the resulting binary image. Given the threshold, the pixels in the gray scale image were assigned a value of ON (or 1) if greater than the threshold value; OFF (or 0) otherwise. The resulting image is a binary image in which blacks denote mastic and whites denote aggregate. Mastic in the context of asphalt is a composite of matrix and fine particulates. The overall composite structure is therefore hierarchical.

To investigate the effect of percent aggregate on the shear modulus G of the asphalt mixes two different image processing techniques were used to produce digital mixes with various aggregate content. The first technique, erosion, is a digital operation performed on binary images where background pixels usually have a value of zero (OFF) and the object or foreground pixels have a value of one (ON). Erosion [16] simply ''peels off'' a layer of predetermined thickness around each particle of aggregate using MATLAB software (Fig. 4). As a result while some aggregates disappear others become smaller. The progressive erosion method via particle removal also uses erosion to avoid the arbitrary change of size of large particles, an alternate erosion technique (using IMAQ Vision software [17]) was used. In this technique, if the particle does not disappear after specified number of erosions it is restored back to its original shape. This means that only the smallest particle aggregates are eliminated at every step until the required concentration is reached. This technique simulates the removal of small aggregates which could be realistically produced in the production of asphalt mixtures.

Finite Element Analysis. The digital cross-section images of a sample of hot mix asphalt (HMA) prepared in the lab using a gyratory compactor were converted to finite element mesh such that each pixel represents one finite element [18]. This ensured that the image and the finite element mesh are identical with respect to the resolution and accuracy. The full mesh contains 344,064 elements in a 512 by 672 grid. A magnified view of a portion of the finite element mesh for the smallest particles is shown in Fig. 5. The finite element analysis was conducted using the ABAQUS computer package [19]. Elements used for meshing were four node plane strain isoperimetric elements (CPE4) with full integration option. The analysis was conducted under plane strain conditions. Typically, an asphalt image has three components to it, namely aggregates, mastic (binder plus dust) and air voids. For this research air voids are ignored and hence the current composite has only two components, mastic and aggregates. Linear elastic properties were used to model both mastic and aggregate phases. Young's modulus was taken to be 50 GPa and 8.23 MPa for aggregate and mastic respectively, based on concurrent experimental work. As for the Poisson's ratio, 0.25 was assumed for aggregate and 0.499 was assumed for mastic. The analyses were run on a dual processor Sun Ultra Sparc 2 workstation.

The conditions of the numerical analysis conducted are as follows. Nodes at the bottom were constrained in both x and y directions. Those nodes on top were constrained only in the vertical direction and were displaced in the horizontal direction. The side boundaries were not constrained. This represents a constant height shear condition. From the reaction forces of the bottom nodes in the horizontal direction, equivalent applied shear stress was calculated. From the constant displacement of the top nodes and the height of the sample, the bulk shear strain were calculated. The shear modulus of the composite was calculated by dividing the ''applied'' shear stress by the ''bulk'' shear strain. It should be noted that since the bulk strain was much smaller than 1%, linear elastic theory is valid, and hence the constraints induced by keeping the height constant can be ignored.

Viscoelastic Analysis. The above finite element analysis is purely elastic. The stiffness G versus volume percent v results were fitted with the following analytical expression.

$$G(v) = A(e^{av} - (v/100)) + (Cv)^n. \quad (2)$$

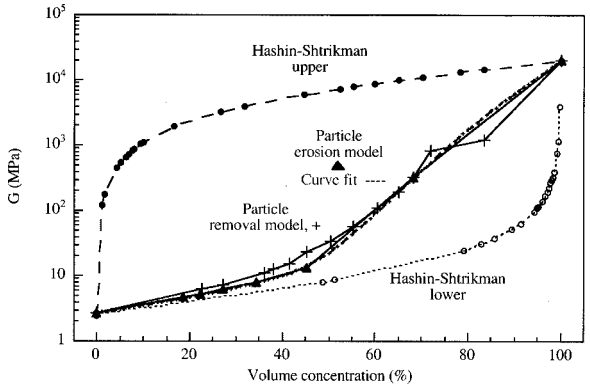

Fig. 6 Elastic behavior of particulate composite as a function of volume fraction, based on FEM. Comparison with the Hashin-Shtrikman bounds.

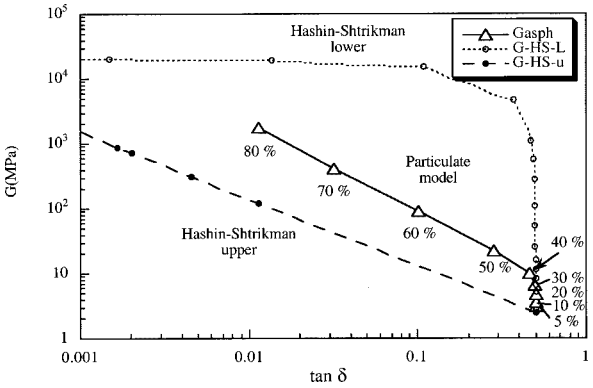

Fig. 7 Viscoelastic behavior of particular composite as a stiffness-loss map with the viscoelastic results of the Hashin-Shtrikman formulas for comparison

Curve fitting (with G in MPa) produced $A=2.74$, $C=0.024596$, $n=11$. This was done only for the erosion model since the particle removal model gave a less regular curve as described below. To obtain viscoelastic properties, the dynamic elastic-viscoelastic correspondence principle was applied to that expression. The correspondence principle provides a solution to a viscoelastic boundary value problem, given a solution to the corresponding elastic boundary value problem. As input to the model, $C=0.024596$ $(1+10^{-4}$ i) was chosen to model the low damping of the particulate phase, $a=0.033$, and $A=2.74$ $(1+0.5$ i) was chosen to model high damping in the matrix phase at low frequency or high temperatures. The imaginary part refers to mechanical energy dissipation. The damping tan δ is the ratio of imaginary part to real part.

III Results and Discussion

Elastic Behavior. Elastic behavior as a function of volume fraction is shown in Fig. 6, and is compared with the Hashin-Shtrikman bounds. Results for the erosion model and particle removal model were similar, but the latter gave more irregular results. All results lie between the bounds for three dimensional isotropy. Since the formulation is plane strain, it is not three-dimensionally isotropic. Up to about 40% volume fraction, the composite stiffness exceeds the Hashin-Shtrikman lower formula, but not by much. This behavior is consistent with results of analytical solutions for dilute concentrations of spherical inclusions. Evidently the irregularity of the inclusion shape has relatively little effect at dilute concentrations. Above 40% volume fraction, the composite stiffness becomes significantly greater than the Hashin-Shtrikman lower formula. At dilute concentrations, the particulate morphology gives the smallest composite modulus for given inclusion volume fraction, much less than for fibers or platelets [20]. The present results indicate the comparative inefficiency of reinforcement becomes less severe as the concentration of irregular particles is increased. In many applications, such as in asphalt and in dental composite resins [21–23], an increase in efficacy of reinforcement is usually beneficial, since the objective is a stiff composite. If, however, the objective is to maximize E tan δ, as is the case in damping applications, then a morphology which is inefficient in terms of stiffness for given volume fraction, is beneficial. As for asphalt and dental composites, a fiber or platelet morphology is not used, owing to cost considerations and the need for casting of the composite from a soft state. Therefore, the use of irregular, jagged particles in high volume fraction, as shown in Fig. 2, is sensible.

Viscoelastic Behavior. Viscoelastic behavior as a stiffness-loss map is shown in Fig. 7. Also shown are the viscoelastic results for the Hashin-Shtrikman formulas; they are not in general bounds for the viscoelastic stiffness loss map, but they are either identical to or close to the true bounds. The finite element results are close to the Hashin-Shtrikman lower formula for a relatively small concentration of particles, 40% or less, and deviates considerably from the lower formula at higher concentration.

For high performance damping layers for absorption of vibration, the figure of merit is the product E tan δ, high values of which appear in the upper right of Fig. 7 (also see Fig. 1 which shows properties of various materials), therefore a composite obeying the Hashin-Shtrikman lower formula gives the best performance. A morphology which gives rise to this behavior is inefficient in terms of stiffness for given volume fraction. The present results show that achievement of high concentration of particles via an irregular morphology results in lower performance than the theoretical maximum. Recall that the Hashin-Shtrikman lower formula for bulk modulus can be exactly attained by the hierarchical coated spheres morphology, and the one for shear modulus is exactly attained by a hierarchical laminate morphology.

In asphalt and dental composites [24], excessive creep is usually undesirable. Since the rate of creep is proportional to the damping tan δ, the present results show the jagged morphology at high concentrations to be beneficial in reducing creep in comparison with a more rounded morphology such as that of coated spheres.

IV Conclusion

For small particle volume concentration 40% or less, the results are close to the Hashin-Shtrikman lower formula in a stiffness vs. concentration plot and in a stiffness loss map. For larger concentration, stiffness is higher and E tan δ is lower. The irregular particle shape therefore enhances stiffness at a given concentration, and reduces damping layer performance.

Acknowledgment

Support to R.S.L. by CMS-9896284, from NSF, and the Mathematical Sciences Research Institute, and support to H. B. via the Federal Highway Administration and the Asphalt Institute are gratefully acknowledged.

References

[1] Delaware Composites Design Encyclopedia. Reviewing editors, L. A. Carlsson, J. W. Gillespie, Jr. Vol. 2, Micromechanical Materials Modeling. J. M. Whitney, R. L. McCullough, eds. Publisher: Technomic, Lancaster, PA, 1989.
[2] Lesueur, D., Gerard, J. F., Claudy, P., Letoffe, M. M., Planche, J. P., and Martin, D., 1996, "A Structure Related Model to Describe Asphalt Linear Viscoelasticity," J. Rheol., **40**, pp. 813–836.
[3] Chen, C. P., and Lakes, R. S., 1993, "Analysis of High Loss Viscoelastic Composites," J. Mater. Sci., **28**, pp. 4299–4304.
[4] Brodt, M., and Lakes, R. S., 1995, "Composite Materials Which Exhibit High

Stiffness and High Viscoelastic Damping,'' J. Compos. Mater., **29**, pp. 1823–1833.
[5] Hashin, Z., and Shtrikman, S., 1963, ''A Variational Approach to the Theory of the Elastic Behavior of Multiphase Materials,'' J. Mech. Phys. Solids, **11**, pp. 127–140.
[6] Read, W. T., 1950, ''Stress Analysis for Compressible Viscoelastic Materials,'' J. Appl. Phys., **21**, pp. 671–674.
[7] Gibiansky, L. V., and Milton, G. W., 1993, ''On the Effective Viscoelastic Moduli of Two Phase Media, I. Rigorous Bounds on the Complex Bulk Modulus,'' Proc. R. Soc. London, **440**, pp. 163–188.
[8] Gibiansky, L. V. and Lakes, R. S., 1993, ''Bounds on the Complex Bulk Modulus of a Two-Phase Viscoelastic Composite with Arbitrary Volume Fractions of the Components,'' Mech. Mater., **16**, pp. 317–331.
[9] Gibiansky, L. V., and Lakes, R. S., 1997, ''Bounds on the Complex Bulk and Shear Moduli of a Two-Dimensional Two-Phase Viscoelastic Composite,'' Mech. Mater., **25**, pp. 79–95.
[10] Zaghloul, S. M., White, T. D., and Kuczek, T., 1994, ''Use of Three-Dimensional, Dynamic, Nonlinear Analysis to Develop Load Equivalency Factors for Composite Pavement,'' Transp. Res. Rec., **1449**, pp. 199–208.
[11] Uddin, W., Zhang, D., and Fernandez, F., 1994, ''Finite Element Simulations of Pavement Discontinuities and Dynamic Load Response,'' Transp. Res. Rec., **1448**, pp. 100–106.
[12] Mamlouk, M. S., and Mikhail, M. Y., 1998, ''Concept for Mechanistic Based Performance Model for Flexible Pavements,'' Transp. Res. Rec., **1629**, pp. 149–158.
[13] Park, J. B., and Lakes, R. S., *Biomaterials*, Plenum, 1992.
[14] Cannon, M. L., 1988, ''Composite Resins,'' *Encyclopedia of Medical Devices and Instrumentation*, J. G. Webster, ed., Wiley, New York.
[15] Papadogiannis, Y., Lakes, R. S., Petrou-Americanos, A., and Theothoridou-Pahini, S., 1993, ''Temperature Dependence of the Dynamic Viscoelastic Behavior of Chemically and Light Activated Composite Resins,'' Dent. Mater., **9**, pp. 118–122.
[16] an Loan, C. F., 1997, *Introduction to Scientific Computing, A Matrix Vector Approach Using MATLAB*, Prentice Hall Inc.
[17] National Instruments, 1996, ''Bridge VIEW and LabVIEW, IMAQ Vision for G Reference Manual,'' Part No. 321379A-01, Oct.
[18] Kose, S., Guler, M., and Bahia, H. U., ''Distribution of Strains within Asphalt Binders in HMA Using Imaging and Finite Element Techniques,'' Presented at the Transportation Research Board 76th Annual Meeting, Jan., 2000, Washington, D. C. and accepted for publication in TRB Records for 2000.
[19] ABAQUS, 1998, *A Finite Element Package*, Version 5.8, Hibbitt, Karlsson & Sorensen.
[20] Christensen, R. M., 1979. *Mechanics of Composite Materials*, Wiley, New York.
[21] Whiting, R., and Jacobsen, P. H., 1980, ''Dynamic Mechanical Properties of Resin-Based Filling Materials,'' J. Dent. Res., **59**, pp. 55–60.
[22] Rosenstiel, S. F., Land, M. F., and Crispin, B. J., 1998, ''Dental Luting Agents; a Review of the Current Literature,'' J. Prosthet. Dent., **80**, pp. 280–301.
[23] Braem, M., Finger, W., Van Doren, V. E., Lambrechts, V. E., and Vanherle, G., 1989, ''Mechanical Properties and Filler Fraction of Dental Composites,'' Dent. Mater., **5**, pp. 346–349.
[24] Papadogiannis, Y., Boyer, D. B., and Lakes, R. S., 1984, ''Creep of Conventional and Microfilled Dental Composites,'' J. Biomed. Mater. Res., **18**, pp. 15–24.
[25] Lakes, R. S., 1998, *Viscoelastic Solids*, CRC Press, Boca Raton, FL.